Applied Energy 282 (2021) 116166

Contents lists available at ScienceDirect

Applied Energy

journal homepage: www.elsevier.com/locate/apenergy

Open-source modeling of a low-carbon urban neighborhood with high shares of local renewable generation

Sebastian Zwickl-Bernhard *, Hans Auer

Energy Economics Group (EEG), Technische Universität Wien, Gusshausstraße 25-29, E370-3, 1040 Vienna, Austria

ARTICLE INFO

Keywords:
Energy technology portfolio
Urban neighborhood
Local renewable energy
Open-source
Geothermal sources
District cooling

ABSTRACT

The main research question of this work is how an urban neighborhood can optimally exploit its local renewable generation potential to cover its electricity, heat and cooling demand. Various cost-minimizing energy technology portfolio studies are examined for an energy community in Vienna, Austria. The method applied is a tailor-made extension of the existing open-source model *urbs*. Additional functionalities and energy services have been implemented. The results of three scenarios identify a variety of different trade-offs between energy technology utilization, local supply within the community and external supply from outside. The introduced performance indicators reveal the respective strengths/weaknesses of the different energy supply options. In this context, the economic efficiency of geothermal sources and the connection to the district cooling network are highlighted, which have so far received little attention. The insights achieved in this work directly support sustainable urban energy planning. Future work may focus on mapping higher spatial resolution, further enhancement of the performance indicators and implementation of operational energy scheduling and dispatch into the open-source modeling approach.

1. Introduction

By 2050, the proportion of humans living in cities is estimated to be two-thirds of the global population [1]. This development increases the complexity of a sustainable energy supply to cover the different energy services in highly populated cities. One possible approach, which takes advantage of synergies in densely populated areas regarding local energy supply, is an energy community (EC) [2]. An EC or small urban neighborhood offers the opportunity to increase the economic use of local renewable energy sources (RES) and technologies, local self-production and the integration of both consumers and prosumers. ECs can not only coincide with the well-known concept of a microgrid but can also be interpreted in a wider context without the need of coherent physical connection of all members of the EC.[1]

Distributed and local energy generation has established itself very strongly over the last decade. In this context, photovoltaic (PV) technology is often mentioned first, but today's technology options are much wider. Exemplarily, small urban neighborhoods provide the opportunity of optimized multiple energy carrier use and offer further synergies in terms of energy generation, consumption, and storage [3]. To cover the demand for electricity, heating, and increasingly cooling multiple energy carriers, however, not only offer synergies, but also may face a competitive constellation between sector coupling technology options [4]. In principle, oversupply for covering the different energy service needs in an EC is possible, as electricity, gas, district heating, and cooling usually can be delivered at the same time if the corresponding infrastructure is available. When taking a holistic approach, these multi-carrier energy distribution networks offer potentials and benefits from both a technical and an economic perspective [5].

However, the implementation of different novel energy technologies enabling sector-coupling at small scale is at the beginning of exploitation only. So, far most studies focus on relatively large regions, so that local-scale benefits remain undetected. The high complexity of small energy systems requires one to incorporate all the key elements on a particular site in detail. Simultaneously, supply from outside and local supply from inside the neighborhood compete with each other and thus affect the characteristics of the most competitive technology portfolio.

The core objective of this paper is to investigate the optimal energy technology portfolio of a low-carbon EC in a small urban neighborhood. In particular, the main research question is how an urban neighborhood can optimally exploit several local renewable generation potentials to cover its electricity, heat and cooling demand, while also taking the existing energy supply infrastructures into account. The distribution grid connection options and possible extensions in the EC play a key role in the optimal technology portfolio composition analysis. Equally

* Corresponding author.
E-mail address: zwickl@eeg.tuwien.ac.at (S. Zwickl-Bernhard).

[1] This terminology as well as the distinction between an energy community and a microgrid is further discussed in Section 2.1 of this paper.

https://doi.org/10.1016/j.apenergy.2020.116166
Received 28 July 2020; Received in revised form 27 October 2020; Accepted 29 October 2020

Nomenclature

Set

$t \in \mathcal{T} = \{1, \dots, T\}$	Timesteps
$p \in \{1, \dots, P\}$	Process
$s \in \{1, \dots, S\}$	Sites
$c \in \{1, \dots, C\}$	Commodity

Variable

ξ	Total annualized system costs (EUR/a)
ξ_{inv}	Total annualized investment costs (EUR/a)
ρ_{ct}	Amount of commodity c at t (t)
κ_p	Total installed capacity per process p (MW)
$\hat{\kappa}_p$	Newly installed capacity per process p (MW)
μ_{pt}	Operational state of process p at t (MWh)
Δ_p^{bdv}	Binary decision variable, true in the case of connection or expansion of process p
ω_t	Weight of timestep t
d_{st}^{elec}	Electricity demand in site s at t (MWh)
d_{st}^{heat}	Heat demand in site s at t (MWh)
d_{st}^{cold}	Cooling demand in site s at timestep t (MWh)
ϑ	Outdoor temperature (°C)
D_s^{Elec}	Annual electricity demand time series in s (MWh)
D_s^{Heat}	Annual heat demand time series in s (MWh)
D_s^{Cold}	Annual cooling demand time series s (MWh)
R_s^{PV}	Annual solar radiation time series in s (MWh)
E_s^{HP}	Annual heat pump efficiency time series in s (MWh)
τ	Time series of characteristic weeks

Parameter

κ_p^{inv}	Specific investment costs per process p (EUR/MW)
Γ_p^{con}	Capacity-independent connection costs (EUR)
κ_{pt}^{var}	Specific variable costs per process p at timestep t (EUR/MWh)
κ_c^{fuel}	Specific fuel costs per commodity c (EUR/MWh)
κ_c^{ext}	Specific costs for external commodity c (EUR/t)

important in the analysis is the identification of synergies and competition between different energy sources, distribution grids, and energy technology options in a small densely populated area.

The method applied to answer the research question is an extension of the existing open-source model (OSM) *urbs* by Dorfner [6]. So far, the model enables optimization for distribution networks (e.g., electricity and heat) with a high temporal resolution and builds the basis of the optimization process. The existing model[2] is a linear program (LP) for capacity expansion planning for multiple energy carriers. In this paper, this model is extended to a mixed-integer linear program (MILP) to consider capacity-independent connection costs (e.g., for district heating and cooling). To reduce the calculation time, tailor-made cluster algorithms are developed for the temporal input data in addition. This enables the representation of annual time series by using characteristic weeks only. Furthermore, the timesteps considered are weighted to enable conversion of the results to annual values again. As an objective function of the optimization problem, both costs and emissions could be minimized [in *urbs]*, with costs being minimized for the results shown in this work.

The case study analyzed is an urban neighborhood in Vienna, Austria. The EC is formed by a university, an office and residential area, a potential new development area and a football stadium. The participants in the EC are selected in such a way as to achieve a high diversity in terms of generation units, load profiles, building structures, and occupancy intensity.

This paper is organized as follows. Section 2 summarizes the current state-of-the-art. In addition, the own contribution beyond the state-of-the-art is outlined. Section 3 presents the methodology and the tailor-made model developed to perform the analysis. Section 4 presents the results of this work for three different scenarios, followed by a sensitivity analysis of key determining parameters in Section 5. Section 6 discusses the results and concludes the work.

2. State-of-the-art

The overview of the state-of-the-art of scientific literature compromises the following subjects: microgrid and EC design aspects, synergies of multiple energy carrier coupling on local level, and the current state of open-source modeling in energy systems. At the end of this section, an outline of the contribution of this work beyond the state-of-the-art is presented.

2.1. Distinction between an energy community and a microgrid

An EC and a microgrid can be distinguished on the basis of the necessity of physical connection within the system boundary of analysis and further conditions in terms of participation. There is no unique definition of microgrids, although in the past it has mainly been seen in the electricity system as a separated part of the low-voltage distribution grid, whereby the functionality and not the size is decisive. Thereby, a microgrid can be connected to the public network or operate separately/remotely. Energy demand is covered by local sources in the microgrid. Microgrids expect both physical connection and mandatory participation of all agents inside the local site to be supplied. In addition, microgrids are optimized from both perspectives, physical and economical [7]. Historically, this approach of isolated systems in the electricity system can be observed in the gradual development of the industry in the United States [8]. An overview of different regional developments is shown in [9]. So far, microgrids have proved that they can deliver benefits and flexibilities when building local clusters of generation, integrating heat and electrical storage, and developing end-user load profiles [10].

In contrast, ECs are not necessarily physically constrained, and participation is voluntary. It is therefore also possible for ECs to define their own rules applied within the boundaries (e.g., different willingnesses to pay of the participants, internal allocation, accounting and billing design) [11]. The participation of individuals in ECs may be economically motivated [12], the desire for purchasing *green electricity* or even the desire for self-sufficiency [13]. In general, ECs can be divided into various groups according to their geographical boundaries [14]: small-scale at the building level; medium-scale at the neighborhood level (clustering of several buildings); and large-scale at the district level.

[2] The model uses the Pyomo package http://www.pyomo.org/ and is solved with the GLPK optimizer http://www.gnu.org/software/glpk/.

The European Commission strongly encourages the development of ECs at different scales. The recently published *Clean Energy Package* promotes ECs, prosumers, and self-consumption and emphatically advocates chances in legislative framework conditions to overcome prevailing obstacles for implementation of these new concepts [15]. A comparison of the regulatory framework conditions in different European countries, as well as suggestions for improvements, is shown in [16]. In addition, there are attempts to recognize ECs as legal entities or so-called *social legal institutions* [17].

Despite the above-described differentiation of the unique characteristics of microgrids and ECs, microgrids can also be understood as and to a large extent coincide with ECs. This frequently is the case. The EC developed in this work also includes several aspects of a microgrid. For example, a connection point to the public electricity, gas, and district heating distribution network exists for the local area and thus is physically bound. However, the consideration of the individual sites in the case study presented in this work as a collaborative structure of prosumers trying to maximize local self-consumption is based on a voluntary basis. Therefore, this particular EC at the neighborhood level is closely related to a microgrid connected to the public distribution grids, albeit it also uses elements of dedicated ECs in a wider context.

2.2. Synergies and modeling of multiple energy carrier systems

Sector coupling on energy systems at different levels and scales has already been analyzed extensively in the literature (e.g., [18,19]). Historically, it is, above all, combined heat and power systems that are worth mentioning here, which in Denmark, for example, have a long tradition in sector coupling and flexibility provision [20]. Optimal technology portfolio integration in multiple energy carrier systems improves the overall energy efficiency, reduces supply costs, and enables the exploitation of local resources and flexibilities of demand [21]. Reliability and flexibility potentials in multiple energy carrier systems are presented in [22]. The potentials to reduce both, costs and emissions compared to traditional energy systems is shown in [23]. In addition, multiple energy carrier systems can deliver various flexibility options over time reaching from rather simple battery storage and demand response supported PV self-generation (see, e.g., review paper [24]) to more complex seasonal energy storage design and modeling [25]. Complex local energy systems in ECs require multidisciplinary modeling approaches capable of mapping not only local generation characteristics but also new energy services (e.g., solar-assisted cooling) [26], end-user behavior and others.

A generic formulation of an optimization model for planning multiple energy microgrids is stated in [27], a more specific approach uses an energy hub at the district level [28]. A combination of energy hubs and distribution grids in one modeling framework is presented in [29]. Residential buildings on local level are considered as a small autonomous energy hub in [30]. Behavioral aspects of agents in an EC and their individual objectives play a major role when designing internal allocation mechanism of an EC. Game theoretical modeling approaches improve the understanding of different levels of cooperative (or non-cooperative) agents' behavior (see, e.g., [31]). In addition, methodological nuances have been addressed in local EC modeling so far. Exemplarily, [32] presents a case study modeling local energy trading at the microgrid level, [33] proposes a cost-effective local emission reduction solution in an urban EC, and [2] elaborates on the trade-offs between energy supply at the micro-district level related to the minimum cost and the minimum emission objective. As also shown later in this work, tailor-made temporal clustering algorithms are developed for the modeling of zero-emission urban neighborhoods in [34]. Furthermore, spatial clustering algorithms taking the existing building structure into account are applied in [2]. Finally, a modeling framework based on a geographical information system for EC studies in a dense neighborhood is presented in [35].

2.3. Open-source energy system modeling

In the past, the lack of open-access modeling has prevented the development of a comprehensive understanding of an energy system model for third parties who were not involved in model development. For outsiders the majority of modeling frameworks are intransparent black or gray boxes [36]. However, open-source modeling has become significantly more important in recent years. Thus further development of models can easily be shared, the implementation of additional functionalities can be accelerated, and new approaches/novelties can easily be contributed to the community [37]. The quality of OSMs is being improved steadily (a possible point of criticism so far) and adaption costs are low. Moreover, the literature presents examples where high-quality modeling can be achieved without significant differences to proprietary software [38]. This also includes open-source energy system modeling [39]. Dorfner demonstrates this with the OSM approach *urbs* on urban entities scale [40]. Subsequently, *urbs* is applied for the energy technology portfolio optimization of urban districts [2]. Besides, *urbs* enables interoperability and the development of platforms for energy systems. Exemplarily, soft coupling with further open-source integrated platforms is shown in a case study in [41]. Comparisons and assessments of *urbs* with two other open-source frameworks are shown in [36]. These comparisons relate to general (e.g., modeling scope and formulation) and specific (e.g., level of detail, and spatial and temporal resolution) aspects in modeling multiple energy systems. Thereby, advanced economic analyses and consideration of the multi-scenario analyses for distributed energy systems are highlighted in *urbs*.

According to [42], FAIR[3] guiding principles can improve management of open-source data. Recommendations for publishing open-source and computer codes are addressed in [43], challenges in the context of reproducibility in [44], and guidelines for data management collaboration in [45].

2.4. Progress beyond state-of-the-art

The contribution of this paper to progress beyond the state-of-the-art addresses the following three dimensions:

First, the methodological approach developed in this work allows to investigate the optimal technology portfolio of a low-carbon EC in a small urban neighborhood under a variety of different settings, constraints and assumptions about the future development of energy services delivered in the community. This includes cost minimized trade-off analyses of both different levels of local renewable self-generation supported by multiple energy carrier coupling technologies and possible extensions of distribution network-based heating and cooling supply from outside the community. Thus, synergies and uneconomic redundancy of different energy technology portfolios can be identified in an EC. In addition, the novel approach serves as a decision support tool for urban energy planning and contributes to answer specific 'what/if' questions in practice. Exemplarily, the question on how best future cooling services can be provided in the community, geothermal-based internal resource extraction versus network-based external district cooling supply, is cited to demonstrate the capability of the approach presented in this work.

Second, the emerging characteristics, determining parameters and interdependent relationships between the different sites of an EC are described by means of dedicated Key Performance Indicators (KPIs)). These EC related KPIs support the discussion and synthesis of results in our work. Exemplarily, the following KPIs are relevant for the EC subject of analysis in this study: local renewable self-reliance; total energy used; total energy purchase from the grid, grid connection capacity;

[3] **F**indable, **A**ccessable, **I**nteroperable and **R**euseable.

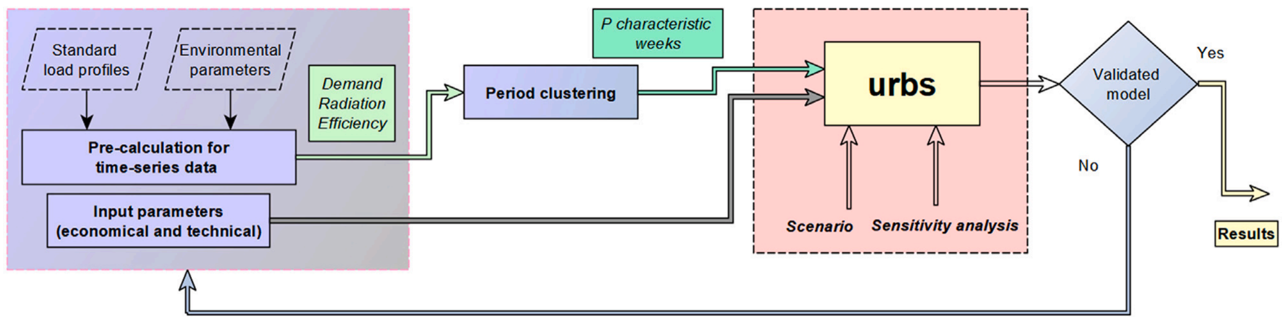

Fig. 1. Flowchart of the modeling approach.

local storage capacities; CO_2 emissions. This list is not exhaustive and can be extended tailor-made for other communities as required.

Third, the tool used to address the research question is OSM. OSM not only contributes to overcoming the black box approach and information asymmetry of third parties in energy system planning and enables better reproducibility of existing studies but also fosters the further development of an OSM in several dimensions and according to the individual needs. In this work, the existing OSM *urbs* is methodologically extended from a LP to a MILP. This enables the consideration of capacity-independent investment costs (e.g., connection to a district heating and cooling network) and further technology-specific characteristics in the EC analysis. These characteristics include the time-dependent efficiency of technologies, exogenous choice of a superior distribution grid infrastructure (e.g., district heating versus gas grid), and weighted time-step modeling (to correctly treat occurrence frequency of parameters that determine technology capacities). Furthermore, empirical and methodological improvements related to data reduction algorithms are implemented to reduce the calculation time in open-source energy system modeling without loss of quality of results.

3. Methodology

This section outlines the methodology applied in this paper. The flowchart of the overall modeling approach is shown in Fig. 1. In Section 3.1 the existing OSM *urbs* is introduced. The description of further improvements of the existing model is shown in Section 3.2. Analytical consideration of the temporal data reduction follows in Section 3.3. In Section 3.4, the case study, the Key Performance Indicators (KPIs) and the corresponding scenarios are defined.

3.1. Existing open-source model (OSM)

The methods of this work are built on the OSM *urbs* by Dorfner [6]. It is a LP, which can be written in the following standard form:

$$\min\, c^T x \quad Ax = b \quad Bx \leq d \tag{1}$$

In the standard form, x is the decision variable vector and c the coefficient vector of the objective function. The matrices A and B as well as the vectors b and d consider the equality and inequality of the mathematical model, respectively. Basically, the model *urbs* is based on the following entities: commodities (represent material and energy flows); processes (convert commodities, e.g., gas to a combination of electricity and heat); transmission lines[4] (transport commodities between sites); storages (store one type of commodity); demand side management.

[4] As already indicated, in this paper the term distribution lines is used instead of transmission lines to highlight the implementation of local ECs on distribution grid level.

Basically, the model provides different objective functions. Either the total costs or the total emissions can be minimized. In this work, the total costs are minimized. Therefore, the objective function can be written as follows:

$$min\ \xi = \xi_{inv} + \xi_{fix} + \xi_{var} + \xi_{fuel} + \xi_{ext} \tag{2}$$

where ξ_{inv} are the annualized investment costs (e.g., processes, distribution lines, and storages), ξ_{fix} the annual fixed costs, ξ_{var} the variable costs, ξ_{fuel} the fuel costs, and ξ_{ext} the external costs per year. The total costs for environmental pollution (external) can be seen as a representation of CO_2 costs.[5] The decision variable vector in the optimization model has the following form:

$$x^T = (\xi, \rho_{ct}, \kappa_p, \hat{\kappa}_p, \mu_{pt}, \epsilon^{in}_{cpt}, \epsilon^{out}_{cpt}) \tag{3}$$

where ξ are the total annualized system costs, ρ_{ct} the amount of commodity c at timestep t, κ_p the total installed capacity per process p, $\hat{\kappa}_p$ the newly installed capacity per process p, μ_{pt} the operational state of process p at timestep t. ϵ^{in}_{cpt} and ϵ^{out}_{cpt} are the total inputs and outputs of commodities per process p at timestep t respectively. Consequently, the objective-function coefficient vector c for minimizing the annual total costs is given as

$$c = (1, 0, 0, 0, 0, 0, 0) \tag{4}$$

3.2. Further improvements of the existing model

This section shows the extension and improvements of the existing model. As a result, the LP is extended to a MILP. To reduce calculation time, annual time series are clustered and represented through characteristic weeks.

3.2.1. Capacity independent connection costs

Investment costs are crucial indicators whether or not technologies are chosen. Consequently, they significantly determine the energy technology portfolio. In the following, the investment costs are extended with a capacity-independent cost driver, which takes connection costs to an existing supply infrastructure into account (e.g., district heating or cooling network). Using the annuity method, investment costs are given as

$$\xi_{inv} = \sum_{p \in P_{exp}} f_p \cdot \{\kappa^{inv}_p \cdot \hat{\kappa}_p + \Gamma^{con}_p\} \tag{5}$$

where f_p is the annuity factor, κ^{inv}_p the specific investment costs per capacity, $\hat{\kappa}_p$ the newly installed capacity, and Γ^{con}_p the capacity-independent connection costs per process p in the subset P_{exp}. This subset collects all processes that are actually expanded. The connection costs are considered in the case of a connection to the network only (e.g., to the district heating network). The decision variable

[5] The concept of external costs introduced in this paper excludes remaining externalities such as NO_X, CH_4 and others.

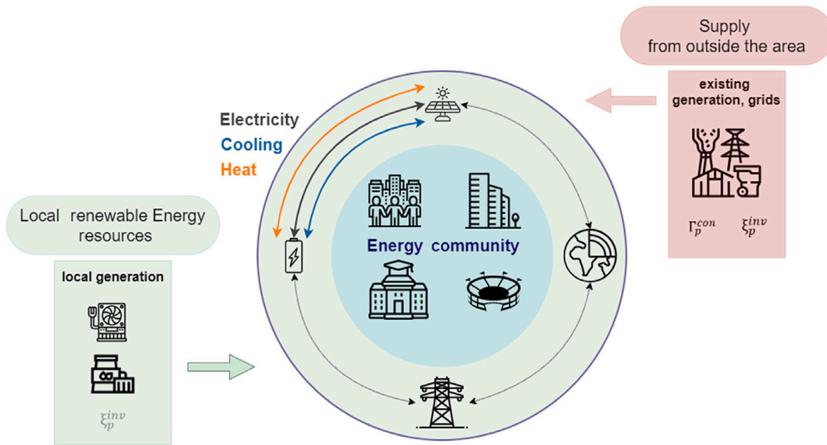

Fig. 2. Energy community and its supply from local renewable energy and from outside.

vector x is extended with binary decisions due to the consideration of capacity-independent connection costs as follows:

$$x^T = (\xi, \rho_{ct}, \kappa_p, \hat{\kappa}_p, \mu_{pt}, \epsilon^{in}_{cpt}, \epsilon^{out}_{cpt}, \Delta^{bdv}_p) \tag{6}$$

where Δ^{bdv}_p are the binary decision variables, which consider whether a process p is newly installed and connected or not. The following constraint sets Δ^{bdv}_p for each process p accordingly:

$$\kappa_p \leq \Delta^{bdv}_p \cdot \bar{K}_p \tag{7}$$

where $\bar{K}_p$ represents the upper bound for the installed capacity per process p.

3.2.2. Exclusive use of gas or district heating

To respect practice-oriented investment decision making in energy distribution grid planning at the district level in municipalities, either gas or district heating is enabled to supply a site in the EC. Therefore, the following constraint is added to highlight the importance of investment decisions when considering the exclusive use of micro combined heat and power (mCHP) or district heating:

$$\Delta^{bdv,s}_{dh} + \Delta^{bdv,s}_{mCHP} \leq 1 \tag{8}$$

where $\Delta^{bdv,s}_{dh}$ represents the binary decision variable as to whether the site s is connected to the district heating network. $\Delta^{bdv,s}_{mCHP}$ takes into account whether a gas-fired process is installed at site s. Fig. 2 helps to illustrate the above-introduced mathematical formulation of the optimization model.

3.2.3. Weighting of timesteps

The existing model allows a high temporal resolution of energy system modeling on an hourly basis. In this analysis, each timestep of the input time-series in the optimization model is extended with a weight. By weighting the individual timesteps, the frequency of a state of the system at the corresponding timestep is considered in the objective function. This extension of the model allows one to calculate the total annual costs without having to consider the full annual time series as input data in the modeling. A detailed description of the reduction concept is given in Section 3.3. The weight of a timestep affects the objective function due to the time-dependency of the variable, fuel, and external costs. Therefore, the components of the objective function can be written as follow

$$\xi_{var} = \sum_{p \in P} \sum_{t \in T_m} w_t \kappa^{var}_{pt} \cdot \mu_{pt} \quad \xi_{fuel} = \sum_{c \in C} \sum_{t \in T_m} w_t \cdot \kappa^{fuel}_c \rho_{ct} \tag{9}$$

$$\xi_{ext} = -\sum_{c \in C} \sum_{t \in T_m} w_t \cdot \kappa^{ext}_c CB(c,t) \tag{10}$$

where w_t is the weight, κ^{var}_{pt} the specific variable costs per process p, κ^{fuel}_c the specific fuel costs per commodity c, κ^{ext}_c the specific costs for external commodities c (e.g., CO_2), and CB the commodity balance (emission level) of the externalities at timestep t in the corresponding subset T_m.

3.3. Temporal data reduction

3.3.1. Pre-calculation of annual time series

The annual time series of the electricity demand are based on standardized load profiles[6] α_i. The heat demand is a measured standardized district heating load profile of the district heating network of the city of Vienna, Austria. The annual time series can, therefore, be written as follows:

$$d^{elec}_{st} = \sum_i \alpha_{it} \cdot \hat{d}^{elec}_{si} \quad d^{heat}_{st} = \beta_t \cdot \hat{d}^{heat}_s \tag{11}$$

where α_{it} represents the standardized electricity load profile, $\hat{d}^{elec}_{si}$ the peak load of customer i at site s, β_t an existing district heating load profile and $\hat{d}^{heat}_s$ the peak load of heat demand of site s. The annual time series of the cooling demand are generated by considering the outdoor temperature (ϑ) as follows:

$$d^{cold}_{st}(\vartheta(t)) = \frac{1}{1 + \exp \frac{-\vartheta + \vartheta_0}{c}} \cdot \hat{d}^{cold}_s \tag{12}$$

where $\hat{d}^{cold}_s$ is the peak load of the cooling demand at site s. In this equation, the cooling demand profile can be influenced by selecting the parameters ϑ_0 and c. Thus, the cooling demand can be determined by factors describing the building structure. ϑ_0 describes a specific outdoor temperature level at which the normalized cooling profile can be set to a half.[7] However, the empirical approach in Eq. (12) excludes temporary thermal storage capabilities of buildings. To consider them only a cutout of the calculated annual cooling demand time series is used as input for the model.[8]

[6] Standard load profiles are representative load profiles that allow a simplified description of the demand of different customer groups (e.g. household, business, industry, etc.).

[7] This is based on assumptions made by empirical studies of thermal profiles that allow a correlation between outdoor temperatures and the corresponding standardized heat demand. Mathematically, this corresponds to the disappearance of the exponent in Eq. (12).

[8] The cooling demand outside the period between June and September is set to zero. Temporary high temperatures in the transition period, which would trigger a significant cooling demand according to Eq. (12), are filtered out.

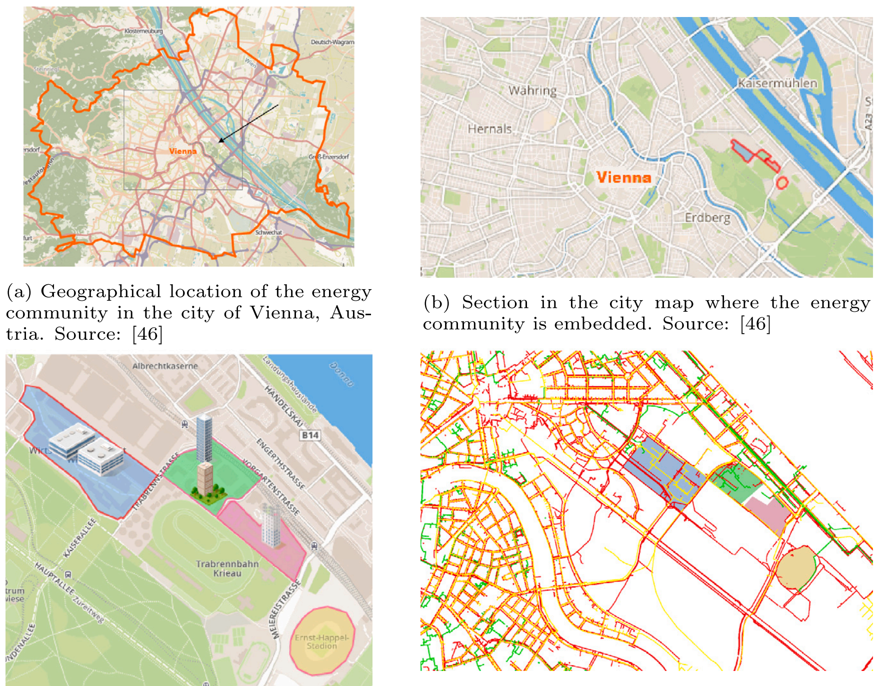

(a) Geographical location of the energy community in the city of Vienna, Austria. Source: [46]

(b) Section in the city map where the energy community is embedded. Source: [46]

(c) Side by side location of *V2* (green), *UNI* (blue), *NEW* (magenta), and *STA* (yellow). Source [46]

(d) Existing distribution grid of gas (yellow), district heating (green) and electricity (red) in the urban neighborhood and its surrounding area. Source: [47]

Fig. 3. Overview of the geographical location of the energy community and the existing distribution grid at the small urban district *Viertel2*. (See [46,47]). (For interpretation of the references to color in this figure legend, the reader is referred to the web version of this article.)

3.3.2. Period clustering algorithm

The analysis presented in this work uses the period clustering algorithm *kmeans++*. The algorithm is an optimization with the objective function, which is to minimize the distance between the input data points x and the centroids m_k of the clusters. The number of clusters N has to be set at the beginning of the optimization. The objective function can be written as follows:

$$min \sum_{P} \sum_{x \in P_i} dist(x, m_k) \tag{13}$$

The data points x are represented by annual time series. To obtain the input matrix, the time vectors of demand (D), radiation (R), and efficiency (E) are converted as follows:

$$D_s^{Elec}, D_s^{Heat}, D_s^{Cool}, R_s^{PV}, E_s^{HP} \in \mathbb{R}^{T_w \times W} \tag{14}$$

with $s \in sites$ and T_w timesteps within a week. Thus, the input matrix M is:

$$M = \begin{pmatrix} D_{V2}^{Elec} & \cdots & D_{NEW}^{Elec} \\ \vdots & \ddots & \vdots \\ E_{V2}^{HP} & \cdots & E_{NEW}^{HP} \end{pmatrix} \tag{15}$$

The results of the clustering algorithm are optimized characteristic weeks with minimal distance to the input weeks. At the same time, each characteristic week is assigned a weight corresponding to its frequency of appearance. The following equation describes this correlation:

$$w_j = \sum_i \Phi_i \text{ with } \Phi_i = \begin{cases} 1 & \min(dist(w_i', \tau)) = dist(w_i', \tau_j) \\ 0 & \text{otherwise} \end{cases} \tag{16}$$

where τ represents the time series of each characteristic week. Φ_i is set to one if the characteristic week τ_j has the minimal distance to the week w_i', otherwise to zero. Hence, the weight w_j describes the number of weeks in a year with the minimal distance to the corresponding characteristic week τ_j. The total of all weights w of the characteristic weeks τ has to be W weeks again. Weights w_j are assigned to the corresponding weight of the timestep t as follows:

$$w_t = \begin{cases} w_j & t \leq T_w \\ w_{j+1} & T_w < t \leq (j+1)\, T_w \\ \vdots & \vdots \\ w_N & (N-1)\, T_w < t \leq N\, T_w \end{cases} \tag{17}$$

The number of characteristic weeks (clusters) has to be selected ex-ante.[9] The algorithm is implemented iteratively to ensure the stability of results indicated as convergence under the following two conditions.

$$\frac{max\ D_s^{demand}}{max\ \tau_j|_{j=\{demand,s\}}} \approx 1 \qquad \sum_t D_s^{demand} \approx \sum_t \{w_j \cdot \tau_j\}|_{j=\{demand,s\}} \tag{18}$$

The two conditions enable convergence of the algorithm in case of a representation of the peak value and total energy of the annual time series.

3.4. Definition of the case study, KPIs and scenarios

3.4.1. Energy community and infrastructure

In the following, we propose an EC in the city of Vienna, Austria (Figs. 3(a), 3(b)). The methodology described in Section 3 is applied to this small urban district called *Viertel2* and its surrounding area. Hence, we composite a local urban neighborhood based on the modern residential and office buildings area *Viertel2* (*V2*), the *Vienna University of Economics and Business* (*UNI*), a new building area currently in the development stage (*NEW*), and the football stadium *Ernst-Happel* (*STA*). The four individual areas are located side-by-side in this small neighborhood (Fig. 3(c)). The areas subject to analyses can be described based on the following characteristics relevant for energy system modeling, whereby the individual characteristics can

[9] This can be seen as a disadvantage of the *kmeans++* algorithm.

Table 1
Relation between inputs and outputs of the energy technologies.

Process	Commodity	Direction	Ratio	Process	Commodity	Direction	Ratio
Photovoltaics	Solar	In	Variable	Solar thermal	Solar	In	1
	Electricity	Out	1		Heat	Out	0.8
Geothermal	Elec	In	1	District heating/cooling	Heat/cold buy	In	1
	Heat/cold	Out	4		Heat/cold	Out	1
	CO_2	Out	0.1		CO_2	Out	0.1
Heat pumps (air–water)	Elec	In	1	mCHP	Gas	In	1
	Heat	Out	Variable		Heat	Out	0.9
	CO_2	Out	0.1		CO_2	Out	0.46
Compression machine	Elec	In	1	Absorption machine	Heat	In	1
	Cold	Out	4		Cold	Out	1
	CO_2	Out	0.1		CO_2	Out	0.13

differ significantly: energy demand (e.g., peak values, total energy demand, and steady versus temporary high consumption); available space for renewable technology integration (e.g., PV systems on rooftops); building structure and building efficiency.

The urban neighborhood runs along and adjoins the recreation and nature reserve *Prater* and, therefore, can be regarded as a self-contained unit. Furthermore, the distribution grids for electricity, gas, and district heating already exist inside or at least on the system border of this neighborhood. This status quo highlights the diverse potential of supply options of this EC with multiple energy carriers (Fig. 3(d)). However, currently there is no direct connection point to the Viennese district cooling network in the immediate vicinity of the area. The four individual areas of the EC are described in more detail, related to important characteristics in terms of their energy supply and demand:

Viertel2 (v2). This area consists of modern residential and office buildings as well as small businesses, shops, and restaurants. Furthermore, the head office of an energy company is located here, which has a strong affinity to be supplied by gas/gas-fired technologies. In 2019 7000 people lived and worked here. The supply of this site already takes local renewable resources into account (e.g., testing project of peer-to-peer trading of local PV generation in a multi-apartment building[10]). A gas-fired, heat-driven mCHP and geothermal sources cover heat supply in the area. In parallel, the geothermal unit also delivers parts of the cooling demand. Furthermore, compression machines cover the cooling demand. The building efficiency of the rather new building stock is high. The demand for energy services concentrates on working days.

University (UNI). This area hosts the campus of Vienna University of Economics and Business and consists of nine different buildings. The modern building complex provides high standards in terms of building efficiency. Restaurants and shops are located here as well. Geothermal sources cover major parts of the heat and cooling demand. Furthermore, the campus is connected to the district heating network. Thus, the peak loads of the heat demand are covered by district heating. Compression machines exist to cover the cooling demand occurring throughout the year (e.g., cooling of the server rooms even in winter).

New building area (NEW). This site enables an expansion of the residential area in the urban neighborhood. At present, this site is in the development stage and lies idle. It is assumed that the buildings that are built meet high efficiency standards. Local renewable technology implementation enables further local self-generation in the area. Furthermore, the supply of each anticipated energy service in this new area is built from scratch. On the basis of an anticipated future residential area, energy demand is spread over the whole week with a noticeable decrease at the weekend.

[10] The objective of shared PV generation within the building is to maximizes self-consumption among participating residents.

Football stadium (STA). This area hosts the *Ernst-Happel* football stadium. Several office buildings are integrated here. The demand for energy services occurs sporadically over the year. In the case of an event (e.g., football matches and concerts), peak electricity loads rise, especially on the weekends. District heating covers the heat demand of the office buildings. Outside event times, the demand for energy services is significantly lower than in the remaining areas of the EC. However, the rooftop of the stadium offers a large space for PV system installations currently not used.

3.4.2. Key Performance Indicators (KPIs)

The description of an EC based on specific KPIs is another innovation of this work. Moreover, dedicated KPIs allow for a systematic characterization and qualitative classification of an EC. This approach can basically be used for several different types of an EC. The KPIs identified in this case study are tailored to the specific Vienesse test bed and do not claim to be complete. In particular, the following KPIs are used:

- *Local renewable self-reliance* represents the amount of locally produced energy inside the community and consumed therein (or stored and consumed at a later point in time).
- *Total energy used* includes both energy supply from local resources inside the community and distribution network-based supply from outside.
- *Total energy purchase from the grid* covers the distribution network-based energy supply from outside the community only. In general, the particular EC setup also allows for exporting locally produced excess electricity.
- *Grid connection capacity* describes the maximum value of the grid connection capacity of the electricity, heating and cooling grid.
- *Local storage capacities* determine the total locally installed storage capacities inside the community.
- *CO_2 emissions* incorporate the total CO_2 emissions of the EC's energy supply from both inside and outside.

3.4.3. Empirical scaling and validation of the model

In addition to technical and economical parameters specifying the technologies, the model expects annual time series as inputs. In the following these input parameter settings are briefly summarized.

The empirical scaling of the technical (e.g., efficiency and emission factors) and economical (e.g., investment, connection and operational costs of processes, storage and distribution grid costs) parameters can be found in Appendix A. Unless explicitly stated otherwise, empirical values of these parameters are taken from our own energy technology database [48]. In the following, selected parameters from Table 1 are discussed, which describe the input/output relation of the processes. For the connection costs for district heating and cooling, typical values characterizing urban sites are taken from [48] which in turn correspond to the assumptions made in [49]. Special attention is also paid to the time-dependent modeling of heat pump efficiency. Time series from [48] are used to describe the relationship between outdoor temperature (determines essentially the outputs of heat pump (air–water) under consideration) and efficiency. The assumed efficiency of geothermal sources is also based on empirical studies collected in [48]. These values are comparable with those in [50] and [51], as they describe existing near-surface geothermal sources and groundwater use in urban areas. The specific emissions for district heating and cooling are justified by empirical studies and the fact that in the specific case mainly waste incineration feeds into the district heating grid.

The different annual time series data of energy demand, generation, and conversion efficiency of technologies are described by measured and synthetic data from the year 2016.[11] For validation of the model, the results of the *baseline* scenario (see Section 3.4.4) are compared with existing data from the environmental report of Vienna University of Economics and Business from year 2019 [50] and publicly available data of *Viertel2* from year 2018 [51]. Notably, the electricity and heat demand validation is examined. For details about the validation of the model parameters and the quantitative numbers used for the comparison it is referred to Appendix B.

3.4.4. Definition of the scenarios

In the following, three scenarios are described narratively. The scenario analysis shall bring further insights into the optimal energy technology deployment and network infrastructure options to supply the EC. Based on dedicated 'what/how if' questions the individual strength and weaknesses shall become visible. To meet practical urban energy planning aspects the existing building stock at the three sites V2, UNI, and STA remain the same in all scenarios. The building standards there are already high and at site NEW exclusively low energy building standards are considered.

The *current state of supply scenario (baseline)* builds upon the existing energy supply infrastructure in the EC. It contributes to answer the questions: What is the least cost strategy for further deployment of low-carbon energy technologies if building upon an inherent energy supply structure? This scenario and the assumptions made therein also validate the model and provide a reference for the remaining scenarios.

The *district heating network scenario* advocates the extension of the district heating network in the urban neighborhood. It addresses the important practical planning question: How best to support energy service coverage in the EC with network-based supply form outside if community internal potentials are limited (e.g., geothermal resources) and/or not competitive? Or the highly controversial question: What are the implications for the remaining energy technology portfolio in the EC if network-based supply alternatives from outside like gas would be even more competitive but not desired due to environmental concerns? The significance of this scenario becomes even more apparent if a municipal waste incineration plant feeds into the district heating network and overarching policies also must be considered.

The *greenfield scenario* not only contributes to the question: What would be the theoretical optimum of an energy technology portfolio and/or a network infrastructure to supply the EC if building them from scratch would be possible? It also supports public relations work in urban development planning. More precisely, by using the different EC related KPIs introduced above this scenario can serve as a reference for a quantitative gap analysis (and justification) of constraint practical achievements compared to a theoretical optimum. In addition, this scenario also provides valuable insights into changing supply shares of the various market actors covering the different energy services.

[11] Sources: electricity profiles [52], heat profiles [53], solar radiation time series [54], temperature time series [55], heat pump efficiency and generation [56], retail electricity, gas and heat prices from the Austrian Regulation Authority [57].

4. Results

This section presents and discusses the results of the case study scenario analysis. Section 4.1 shows the highlights of the *current state of supply scenario (baseline)*, Section 4.2 the *district heating network scenario*, and Section 4.3 the *greenfield scenario*. Section 4.4 compares the results of the different technology portfolios in the three scenarios under special consideration of the EC related KPIs introduced in the previous section.

4.1. Current state of supply scenario (baseline)

The amount of total energy produced for covering electricity, heat and cooling demand by technology and site within the EC is shown in Fig. 4.

Electricity. A significant proportion of electricity demand is covered by external electricity purchases from the grid and account for more than 80 % of the total annual costs. Electricity purchase mainly supplies the electricity demand at *UNI*. The remaining electricity is delivered from local PV generation in the neighborhood. With the exception of a small share of already existing PV capacities at *V2*, several remaining PV capacities are newly built. The combination of a high demand for electricity and comparatively low selling prices for excess PV generation to the grid results in high shares of local self-consumption. PV electricity generation on *STA* significantly exceed the electricity demand at this site and therefore is consumed in the neighboring sites of the EC.

Heat. The heat demand of the EC is mainly covered by geothermal sources. Whereas *V2* and *UNI* are supplied with the already existing geothermal energy facilities, *NEW* expects new geothermal capacity installations. In addition, the two sites connected to the district heating network, *UNI* and *STA*, are supplied from outside the urban neighborhood. *STA* is supplied exclusively with district heating, whereas at site *UNI* it is used to cover peaks in heat demand only. The local mCHP supplies the heat peak demand in *V2*.

Cooling. The entire cooling demand is covered by geothermal capacities for cooling and compression machines. The use of these two technologies underlines the importance of electricity for delivering cooling services. Generation capacity structures covering cooling demand are identical both in areas with (*V2* and *UNI*) and without (*NEW*) initial capacities. The low demand for cooling at *STA* is also covered by geothermal sources.

Fig. 5 shows a high temporal resolution of electricity production and demand at *UNI* during the four characteristic weeks. This figure also indicates the interaction between consumption at *UNI* and PV generation at *STA*. The gray area clearly underpins the high share of electricity purchases from the grid. The share of local PV self-production at *UNI* itself (yellow) and the shared contribution from *STA* (green) result in a high share of local PV self-consumption inside the EC. In the first characteristic week (typical week in summer) the PV electricity generation is used to "fuel" the cooling technologies (geothermal devices and compression machines) responsible for covering cooling demand. During the last two characteristic weeks (typical week in winter and week of the year with the highest heat demand) there is almost no local electricity production in the neighborhood. The electricity for the geothermal heating units is almost exclusively purchased from the grid. In the second characteristic week (week in the transition period) almost the entire electricity demand can be covered by local PV generation on weekends.[12]

[12] As a result of the clustering algorithm, the weekend days are represented with day five and six in a characteristic week. This shift of one day (compared to real life) has a mathematical reason and is due to the impact of the submatrices in Eq. (15) on the clusters.

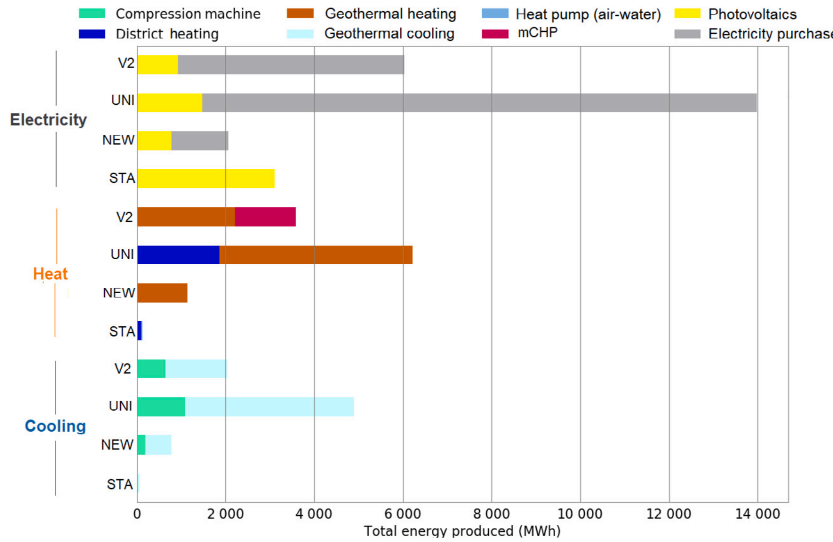

Fig. 4. Total energy produced for covering the electricity, heat and cooling demand in the *current state of supply scenario (baseline)*.

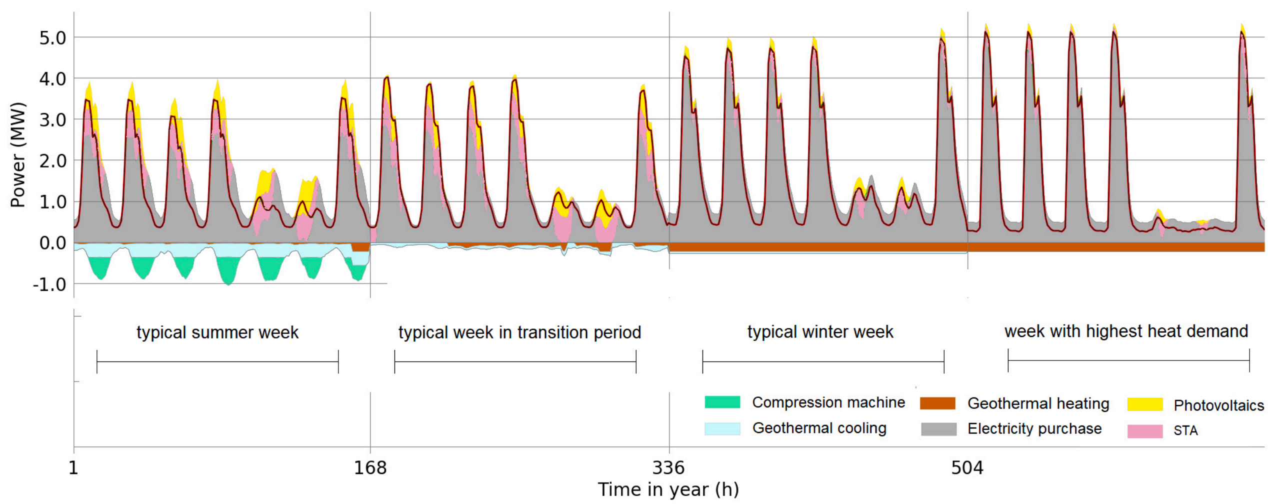

Fig. 5. Temporal resolution of electricity generation and demand at *UNI* during the four characteristic weeks.

The interaction of the individual sites *V2*, *UNI*, and *STA* in the neighborhood is illustrated in Fig. 6. The Sankey diagram reveals the electricity flows to technologies for covering the cooling demand at *UNI* and *V2*. Depending on the respective cooling demand at these sites, geothermal devices or compression machines consume a corresponding higher share of electricity. However, *UNI* has a higher total electricity demand for cooling than *V2*. A significant part of this demand can be met by local PV electricity generation at *STA*.[13]

Technologies. Electricity and heat storage technologies are installed in the EC. At *STA* and *NEW* hydrogen storage is used to increase the flexibilities in the electricity sector. The hydrogen storage at *STA* enables to store and shift the locally generated PV electricity to times at higher energy demand in the EC. This also contributes to the avoidance of distribution grid capacities extensions. The larger share of installed storage capacities are, however, seasonal heat storages.

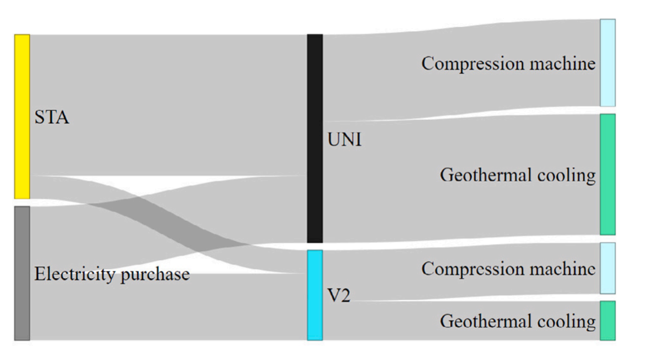

Fig. 6. Electricity flows for covering cooling demand at *UNI* and *V2* in a characteristic summer week.

4.2. District heating network scenario

The focus of this scenario is on the heat supply from outside the urban neighborhood. Thus, a connection of the entire EC (i.e., several of the four sites) to the district heating network is intended to cover

[13] Note that the model neither prefers *UNI* nor *V2* and treats both participants equally in terms of distribution of local produced PV electricity. The same amount of electricity purchases from the grid for both individual areas are assumed. Hence, there is no need to show *NEW* explicitly as 100% of electricity need to be purchased from the grid.

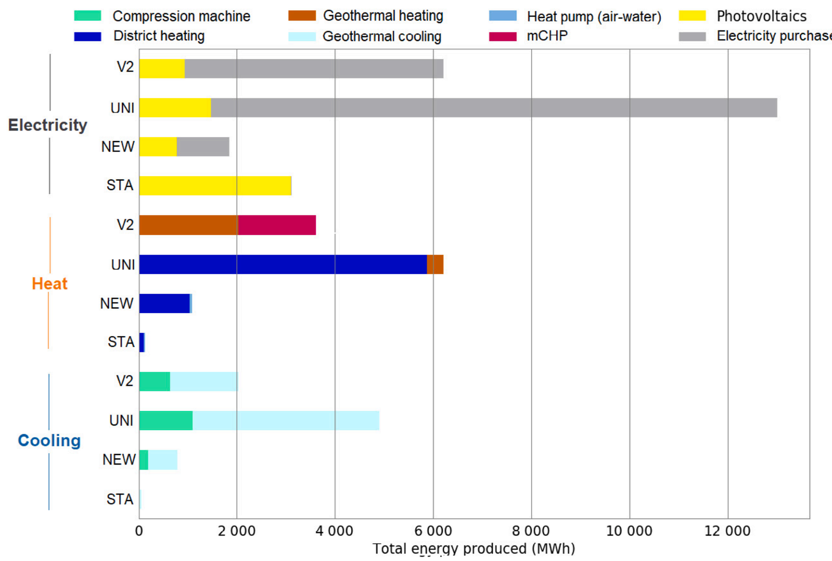

Fig. 7. Total energy produced for covering the electricity, heat, and cooling demand in the *district heating network scenario*.

the heat demand. Two different options are considered and examined: (i) policy decision in municipal energy planning to connect the entire EC with the district heating network, and (ii) extension of the district heating network based on technical and economical considerations.

The first option, which considers the policy decision of expansion planning, shows essentially the same result as in the *baseline* scenario. District heating is used exclusively to cover peak loads in the EC. Geothermal sources still cover the high shares of base load of the heat demand. This is possible due to the high efficiency of geothermal source exploitation in this area. Thus, the capacity-independent connection costs for the district heating network are negligible in the case where geothermal sources and district heating compete in the presence of high local geothermal efficiency.

The second option for district heating expansion shows a significantly different energy technology portfolio. The assumed lower local efficiency of geothermal source exploitation and a reduced district heating price trigger a significantly higher district heating coverage of heat demand in the EC. The results presented in Fig. 7 assume a 15 % lower value of geothermal efficiency.[14] The results of the energy technology portfolio related to a reduced district heating price do not differ significantly and are, therefore, not shown here.

Electricity. In this scenario electricity demand decreases at *UNI* by about 10 %. In the areas *V2, NEW* and *STA*, electricity demand remains the same. This is also the case for local PV capacity installations and PV self-generation.

Heat. The heat supply is mainly delivered by district heating, which covers almost the entire heat demand in the EC (+260 % compared to *baseline*). In addition, low capacities of geothermal sources at *UNI* and heat pumps at *NEW* are installed. These two technologies cover the low heat demand in the transition period week. The heat supply in *V2* remains the same as in the *baseline* scenario (i.e., same proportions of geothermal sources and local mCHP).

Cooling. The cooling demand is supplied by geothermal sources and compression machines as in the *baseline* scenario.

[14] In terms of particularities of local geothermal efficiency see also corresponding explanations in Section 3.4.4.

4.3. Greenfield scenario

In this scenario, the energy supply infrastructure of the EC is assumed to be built from scratch. Hence, the model omits the existing installed energy technologies and distribution network capacities. The investment decision in energy technologies and grid infrastructures is subject of the analysis. Note, that the assumed building stock (especially with regard to building efficiency standards) is the same as in the remaining two scenarios. The corresponding results of the amount of total energy produced for covering electricity, heat and cooling demand in the four different sites within the EC are shown in Fig. 8.

Electricity. The electricity generation is similar to the *baseline* scenario. This includes both local PV self-consumption and electricity purchases from the grid.

Heat. In heat supply the energy technology portfolio is significantly different compared to the remaining two scenarios. Almost the entire heat demand in the EC is covered by geothermal sources. At *UNI*, the peak loads in the heat demand are covered by the district heating network. However, the amount of produced district heating energy is lower than in the *baseline* scenario. Daily heat storage devices are installed in the three areas with exclusive heat supply from geothermal sources. This reduces the necessary capacities of geothermal devices to supply peak loads. Furthermore, no more mCHP is installed to cover parts of the heat demand, as is the case in the *baseline* scenario at *V2*.

Cooling. In the areas *V2, NEW* and *STA* the cooling demand is supplied as in the previous scenarios, even if the share of geothermal cooling is higher. There are significant differences in the way *UNI* is supplied as it is connected to the district cooling network, which covers a high share of the cooling demand there. However, this connection is economical for large cooling demand (*UNI*) only. Owing to the lower demand for cooling in the remaining three areas, electricity still prevails to supply the cooling technologies, which is covered by compression machines and geothermal cooling.

4.4. Comparison of the different scenarios

In the following, the results of the three different scenarios are compared on the basis of both energy technology portfolio (installed capacities per technology) and KPIs. Fig. 9 shows that the installed process capacities vary significantly between the scenarios, notably in terms of supply by district heating and cooling from outside the EC.

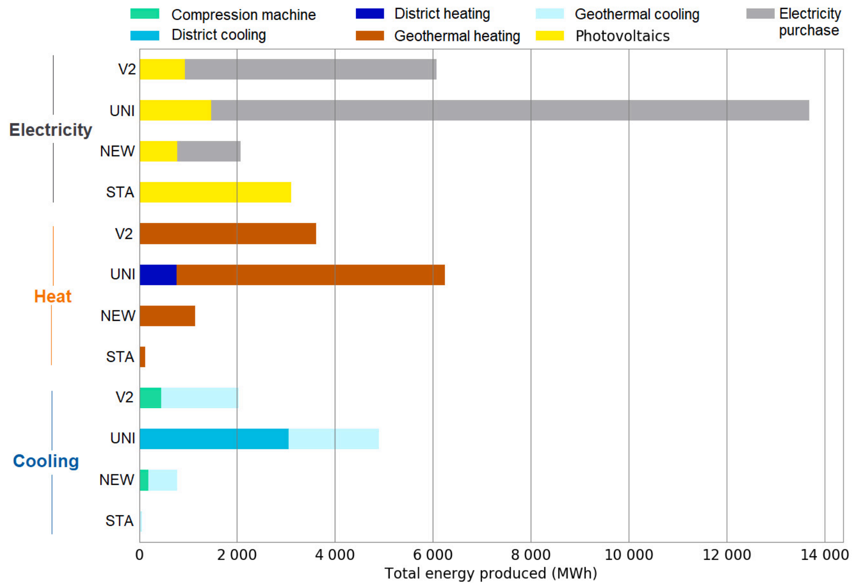

Fig. 8. Total energy produced for covering the electricity, heat, and cooling demand in the *greenfield scenario* (supply from scratch).

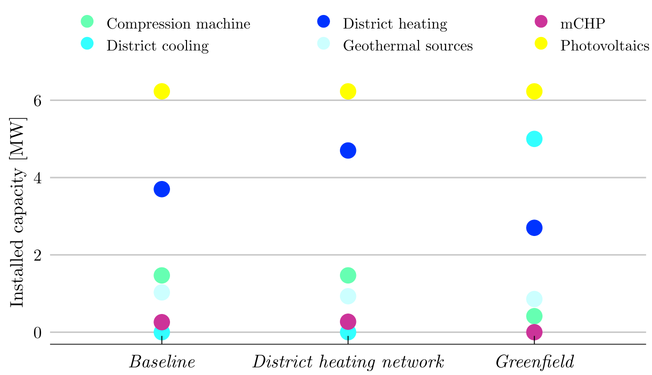

Fig. 9. Overview of the energy technology portfolio in the three scenarios.

The extension of local PV generation capacities remains constant in the three scenarios. Furthermore, absorption machines, heat pumps and solar thermal are excluded from the energy technology portfolio in each scenario. Note, that the main factors excluding these technologies from the investment decision in the energy technology portfolio are as follows: for absorption machines it is the comparatively high energy price for the two inputs required, electricity and heat; for heat pumps it is the non-competitive coefficient of performance (COP) dependent on the outside temperature; and for solar thermal, it is the higher competitiveness of PV qualified to deliver the same energy services. Even if the generated energy differs significantly, the installed geothermal technology capacities remain almost constant in the three scenarios. The supply from scratch favors network-based district cooling and decreases compression machine capacities.

The comparison of the KPIs is shown in Fig. 10 (local renewable self-reliance, total energy used, total energy purchase from the grid, installed storage capacities) and Fig. 11 (total costs (incl. its relevant components), CO_2 emissions). The local renewable self-reliance (shown in absolute values) is almost identical in the *baseline* and *greenfield scenario* and larger than in the *district heating network scenario*. Furthermore, the total energy used in the three scenarios is almost the same. The total energy purchase from the grid and thus supply from outside the EC is highest in *district heating network scenario*. At the same time, the local storage capacities are the lowest in this scenario. Note, that this difference is due to the varying installed capacities of seasonal heat storage, as the installed hydrogen storage capacities are the same in all scenarios.

The total costs are almost identical in the three scenarios. This is due to the fact that electricity purchase accounts for a significant portion of all scenarios. However, the share of investment costs is highest in the *greenfield scenario* and lowest in the *district heating network scenario*. In the latter case, heating purchase costs are the dominant part of the total costs. Finally, the annual CO_2 emission comparison shows that although lower emissions are emitted in the *baseline* scenario than in the *district heating network scenario*, substantially lower emissions occur in case of a potential new supply of the EC from scratch in the *greenfield scenario*.

5. Sensitivity analysis

In this section input parameters are varied to investigate different sensitivities of both energy technology portfolio composition and technology utilization. Notably, the following two sensitivities are of particular interest: varying CO_2 prices and expansion of the district cooling network.

5.1. Varying CO_2 prices

In the following, the effects of increasing CO_2 prices on the energy supply structure of the EC are analyzed for the *baseline* scenario. In quantitative terms, the determination of the changes of installed technology capacities at V2 and NEW are of particular interest. Changes of the energy technology portfolio composition provide further insights into the sensitivity of carbon pricing.

Fig. 12(a) shows the already identified significant share of geothermal sources for heat supply in case of low CO_2 prices. In addition, the currently prevailing low CO_2 prices favor the use of the existing mCHP unit (covering almost 40 % of the heat demand). With an increase in the CO_2 price above 40 EUR/t, the mCHP unit loses market shares to geothermal-based heat supply. At a CO_2 price of 70 EUR/t mCHP completely phases out.

Fig. 12(b) shows the development of the total costs of energy supply in the entire EC for increasing CO_2 prices. Total costs increase with decreasing shares of gas-fired heat-driven mCHP production due to higher heat production costs of geothermal heating. In the case of an almost complete supply of the heat demand in the EC by geothermal sources, the impact of increasing CO_2 prices on the electricity price and thus on the total costs is low.

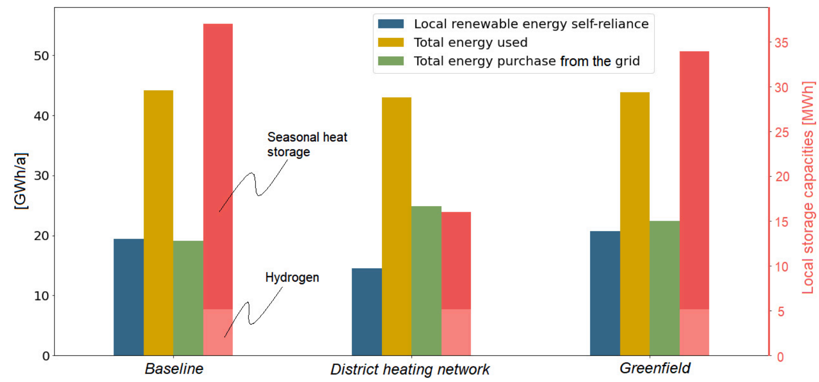

Fig. 10. KPIs showing local renewable self-reliance, total energy used, total energy purchase from grid and local storage capacities in the three scenarios.

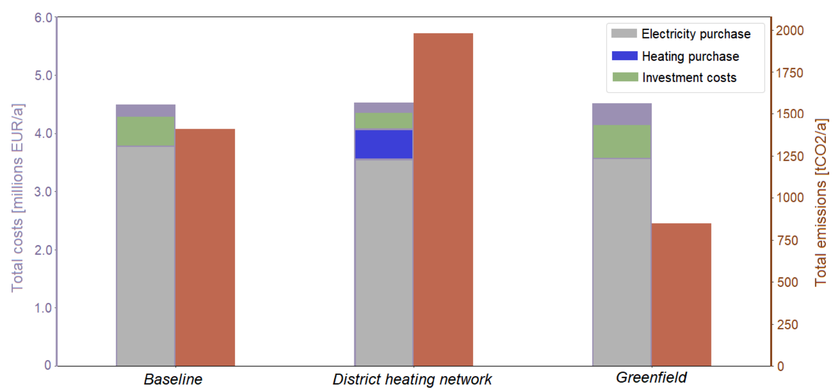

Fig. 11. Total costs (incl. its relevant components) and total CO_2 emissions in the three scenarios.

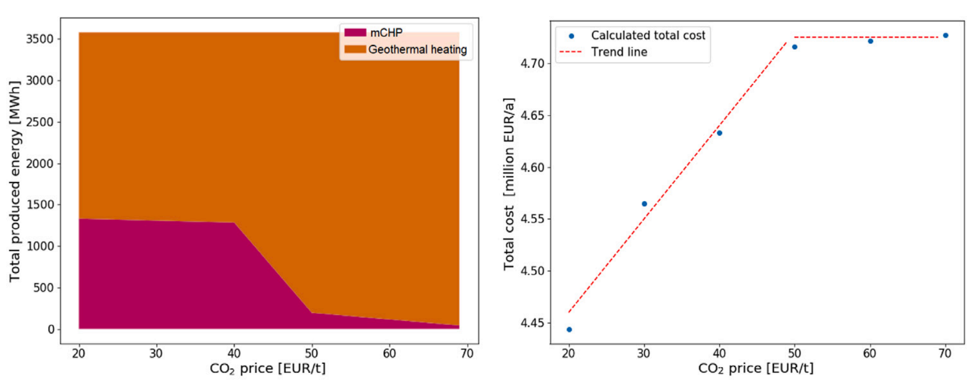

(a) (b)

Fig. 12. (a) Total produced energy for heat supply at *Viertel2* for different CO_2 prices. (b) Total costs of energy supply in the EC for different CO_2 prices.

To better illustrate the so-called *technology lock-in effect*, Fig. 13 compares the technology shares of the heat supply at site *V2* and site *NEW*. The existing gas-fired mCHP capacity at *V2* delivers significantly less total produced energy above a CO_2 price of 50 EUR/t. The results at *NEW* concede a high share of the gas-fired mCHP unit at a CO_2 price of 20 EUR/t and a low efficiency of geothermal source exploitation at this site only.[15] An increased CO_2 price of 30 EUR/t changes the energy technology portfolio in *NEW* already significantly. Then, almost the entire heat demand is supplied by the district heating network. Nevertheless, the higher CO_2 price also decreases the profitability of district heating. However, geothermal sources cannot compete and are not expanded due to the high investment costs. Therefore, district heating supply shows greater robustness in terms of increasing CO_2 prices.

5.2. District cooling: connection costs and district cooling price

In the following, a sensitivity analysis in the *greenfield scenario* investigates the competitiveness of the existing local cooling supply in the community compared with a possible connection of site UNI to the district cooling network currently implemented outside the EC only.

Fig. 14 shows the relation between the distance to the nearest possible district cooling connection point outside the EC and the maximum district cooling price resulting in a competitive cooling supply and connection to the district cooling network. In the blue-marked area, district cooling is more profitable than the alternatively preferred local supply by geothermal sources and compression machines. Outside the

[15] Compare also the assumptions in Section 4.2.

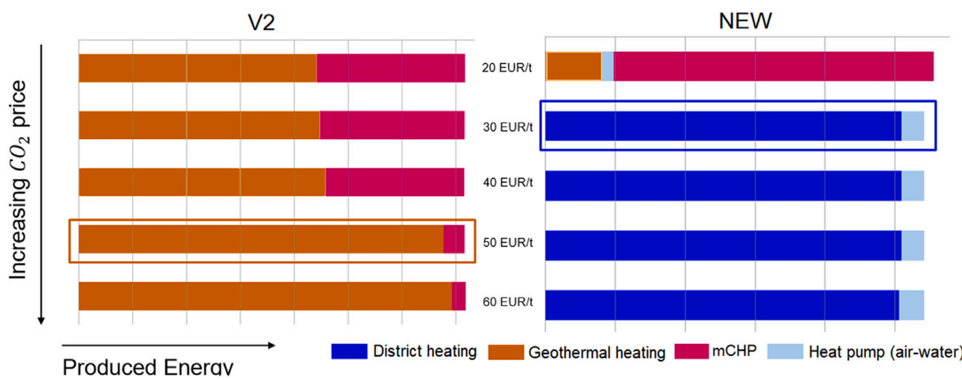

Fig. 13. Comparison of total produced energy for heat supply for different CO_2 prices at *V2* (left) and *NEW* (right).

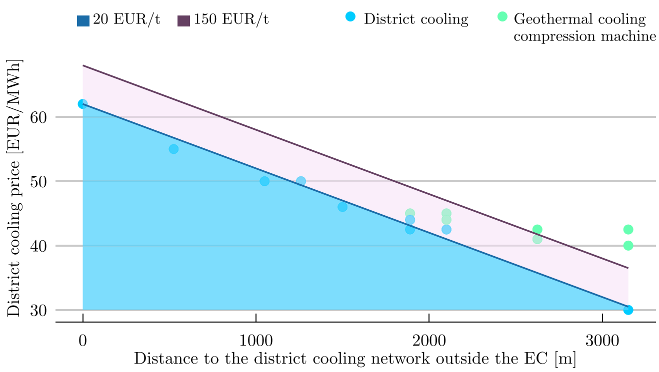

Fig. 14. Profitability limit of the district cooling price in dependence of the distance to the existing district cooling network outside the EC for two different CO_2 prices. (For interpretation of the references to color in this figure legend, the reader is referred to the web version of this article.)

blue-marked area, the EC is supplied by geothermal-based cooling technologies and compression machines. An increasing CO_2 price in Fig. 14 relaxes the competitive connection distance benchmark of the district cooling network and the district cooling price. Thus the profitable area of both parameters increases (see the purple-marked area). Essential for this is the effect of the CO_2 price on the electricity price and thus on the profitability of compression machines and geothermal-based cooling technologies.

6. Conclusions and outlook

This work examines different energy technology portfolios options for a low-carbon energy supply of an urban neighborhood with high shares of local renewable generation. In a Viennese test bed the trade-offs between different energy technologies, local supply from the neighborhood and external supply are investigated for three different scenarios. The investigated scenarios are of particular practical relevance for a novel type of urban energy planning, taking into account environmentally friendly policy implementation.

The introduction of specific Key Performance Indicators (KPIs) has proved successful in systematically describing and assessing an energy community's performance. The KPIs specifically adapted to the case study of this work are a useful tool to compare the strengths and weaknesses of different energy technology portfolios and the corresponding energy network infrastructure needs in the different scenarios. Among others, this provides a deeper understanding of the capability of local renewable energy self-reliance, total energy use and its composition, and the corresponding disaggregated and total costs. It is essential to gain insight into the detailed allocation and breakdown of costs between technologies inside and outside the community and the network infrastructure related share in the provision of energy services in the energy community. This is not least because differences in the composition of the energy supply and thus the allocation of costs in the various scenarios directly influence the pricing and tariff setting of the various market participants and regulatory authorities in practice.

In addition, the case study in this work includes emerging energy services and energy technology options, many of which have received little attention in practice and in the modeling of energy systems so far.

Table A.1
Technical and economical input data of processes in the energy community.

Site	Process	Installed capacity [MW]	Investment costs [EUR/MW]	Fixed costs [EUR/MW]	Variable costs [EUR/MWh]	Weighted average costs of capital [%]	Depreciation [year]	Area per capacity [m^2/MW]	Connection costs [EUR]
V2	Photovoltaics	0.28	850 000	8 500	–	2	20	6500	–
	Solar thermal	–	1 200 000	12 000	–	2	20	1250	–
V2	mCHP	0.25	875 000	26 250	6.4	2	20	–	–
V2	Geothermal (heating)	0.18	1 600 000	32 000	–	2	40	–	–
UNI	Geothermal (heating)	0.2	1 600 000	32 000	–	2	40	–	–
	Heat pumps (air–water)	–	510 000	10 200	0.5	2	20	–	–
UNI	District heating	2.7	–	–	–	2	40	–	300 000
	District cooling	–	–	–	–	2	40	–	1 050 000
V2	Compression machine	0.65	200 000	4 000	–	2	20	–	–
UNI	Compression machine	0.65	200 000	4 000	–	2	20	–	–
	Absorption machine	–	800 000	16 000	–	2	20	–	–
V2	Geothermal (cooling)	0.1	1 600 000	32 000	–	2	40	–	–
UNI	Geothermal (cooling)	0.25	1 600 000	32 000	–	2	40	–	–

Table A.2
Technical and economical input data of storage in the energy community.

Storage	Commodity	Installed capacity [MW]	Cap up of installed capacity [MW]	Efficiency in [1]	Efficiency out [1]	Investment costs [EUR/MW]	Investment costs [EUR/MWh]	WACC [%]	Depreciation [year]
Hydrogen	Electricity	–	–	0.65	0.65	100	25 000	2	25
Battery	Electricity	–	–	0.96	0.96	10 000	500 000	2	15
Day storage	Heat	–	2 000	0.95	0.95	–	5 000	2	30
Seasonal storage	Heat	–	100 000	0.95	0.95	–	1 500	2	40

Table A.3
Technical and economical input data of distribution grid capacities.

Site in	Site out	Distribution	Commodity	Investment costs [EUR/MW]	Fixed costs [EUR/MW]	WACC [%]	Depreciation [year]
UNI	NEW	Low-voltage AC	Electricity	1 650 000	16 500	2	40
UNI	STA	Low-voltage AC	Electricity	1 650 000	16 500	2	40
UNI	V2	Low-voltage AC	Electricity	1 650 000	16 500	2	40
V2	STA	Low-voltage AC	Electricity	1 650 000	16 500	2	40
V2	NEW	Low-voltage AC	Electricity	1 650 000	16 500	2	40
NEW	STA	Low-voltage AC	Electricity	1 650 000	16 500	2	40

Table A.4
Economical parameters and commodity prices.

Commodity	Price [EUR/MWh]	Source
Gas	18	[58]
CO_2	20	[14]
Electricity buy	200	–
Electricity sell	30	–
Heat/Cold buy	50	[49]

In particular, the use of local geothermal sources for the provision of heating and cooling services and the potential connection to the district cooling network outside the community has proven to be competitive and a serious alternative in a future portfolio of energy services offered in the community. The sensitivity analyses, furthermore, examine the profitability benchmarks of geothermal sources and network-based district heating and district cooling supply at different CO_2 prices and connection costs. These insights and results directly support urban development planning and policy-making.

Open-source modeling serves as an essential instrument and tool for carrying out the analysis of the multiple energy carrier system analyses in the Vienna test bed. The strengths of open-source modeling are exploited by enabling a tailor-made extension and implementation of functionalities in existing models that meet the requirements of the case study under investigation. The high quality of the open-source modeling approach also becomes visible in the context of the validation of the model, as it shows comparatively small differences between real and calculated values. Furthermore, it demonstrates that applicability and extendibility for third parties according to specific needs (i.e., spatial and temporal granularity, tailor-made clustering algorithms to achieve adequate simulation time) are possible. Thus open source models deliver added value to the research and modeling community.

Table B.1
Comparison between the real and calculated values of the electricity, heat and cooling demand.
Source: [50,51]

Description	Type	Electricity UNI [MWh/a]	Heating V2 [MWh/a]	Heating UNI [MWh/a]	Cooling UNI [MWh/a]
Demand	Reality	13 056	3 385	5 602	6 954
	Calculated	13 557	3 601	6 254	4 889
mCHP	Reality	–	1 425	–	–
	Calculated	–	1 431	–	–
District heating	Reality	–	–	1 808	–
	Calculated	–	–	2 085	–
Electricity demand heat and cooling	Reality	2 786	–	–	–
	Calculated	2 346	–	–	–

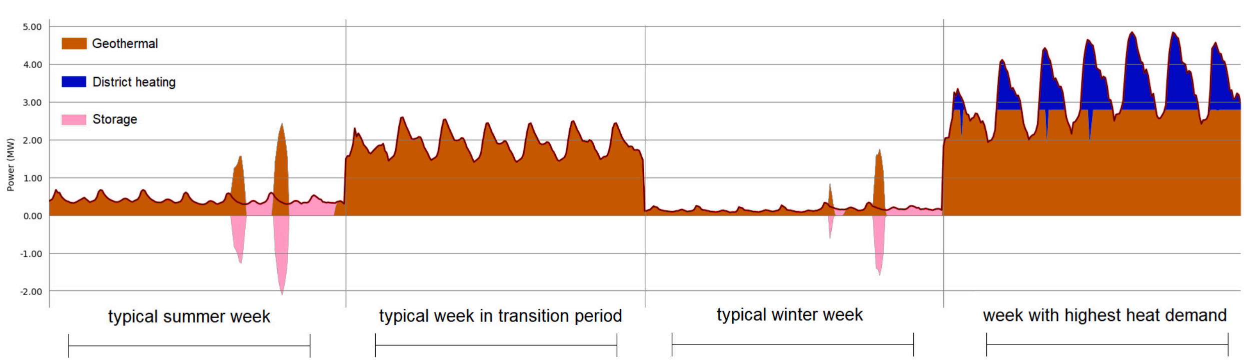

Fig. B.1. High resolution of the heat supply in the current state scenario (*baseline*) at *UNI*.

Future work may include at least the following aspects: an extension of the functionalities of the model, an even higher geographical resolution of the EC and its distribution grids, an enhancement of the KPIs and further operational aspects of prosumers within the energy community. The model can be extended to determine the net present value of different energy technology options. A higher geographical resolution allows to determine the optimal expansion and size of existing and new ECs. The KPIs can be extended in socio-economic or environmental aspects (i.e., total number of prosumers locally supplied, environmental footprint on building level, etc.). Operational aspects may take into account the individual behavior of prosumers, scheduling and load forecast from energy services as well as building integration and shadowing of local PV systems.

CRediT authorship contribution statement

Sebastian Zwickl-Bernhard: Conceptualization, Methodology, Software, Validation, Investigation, Resources, Data curation, Writing - original draft, Writing - review & editing, Visualization. **Hans Auer:** Conceptualization, Validation, Writing - review & editing, Supervision.

Declaration of competing interest

The authors declare that they have no known competing financial interests or personal relationships that could have appeared to influence the work reported in this paper.

Appendix A. Data

See Tables A.1–A.4.

Appendix B. Validation of the model

This section presents the validation of the model. Hence, the electricity, heat and cooling demand is compared between the *baseline* scenario and available data from the individual areas. The data are taken from the environmental report of Vienna University of Economics and Business (UNI) [50] as well as from the published data of the urban area *Viertel2* (V2) [51]. In the following, the produced energy of district heating and the mCHP as well as the electricity demand for heat and cooling are compared (Table B.1). This allows one to validate not only the model itself but also the assumed parameters of the technologies.

As can be seen from the environmental report, district heating covers peak loads of the heat demand. This is also reflected in the high-resolution representation of heat supply in the modeled *baseline* scenario (Fig. B.1).

References

[1] Ritchie H, Roser M. Urbanization. Our world in data. 2018, https://ourworldindata.org/urbanization.

[2] Fleischhacker A, Lettner G, Schwabeneder D, Auer H. Portfolio optimization of energy communities to meet reductions in costs and emissions. Energy 2019;173:1092–105. http://dx.doi.org/10.1016/j.energy.2019.02.104.

[3] Lund H, Østergaard PA, Connolly D, Mathiesen BV. Smart energy and smart energy systems. Energy 2017;137:556–65. http://dx.doi.org/10.1016/j.energy.2017.05.123.

[4] Lazzarin R, Noro M. Local or district heating by natural gas: Which is better from energetic, environmental and economic point of views? Appl Therm Eng 2006;26(2–3):244–50. http://dx.doi.org/10.1016/j.applthermaleng.2005.05.007.

[5] Widl E, Jacobs T, Schwabeneder D, Nicolas S, Basciotti D, Henein S, et al. Studying the potential of multi-carrier energy distribution grids: A holistic approach. Energy 2018;153:519–29. http://dx.doi.org/10.1016/j.energy.2018.04.047.

[6] Dorfner J. Urbs: A linear optimisation model for distributed energy system. 2015, Urbs 0.7, vol. 1. https://github.com/ojdo/urbs.

[7] Soshinskaya M, Crijns-Graus WH, Guerrero JM, Vasquez JC. Microgrids: Experiences, barriers and success factors. Renew Sust Energy Rev 2014;40:659–72. http://dx.doi.org/10.1016/j.rser.2014.07.198.

[8] Marnay C, Venkataramanan G. Microgrids in the evolving electricity generation and delivery infrastructure. In: 2006 IEEE power engineering society general meeting. IEEE; 2006, p. 5. http://dx.doi.org/10.1109/PES.2006.1709529.

[9] Ali A, Li W, Hussain R, He X, Williams BW, Memon AH. Overview of current microgrid policies, incentives and barriers in the European union, United States and China. Sustainability 2017;9(7):1146. http://dx.doi.org/10.3390/su9071146.

[10] Marnay C, Venkataramanan G, Stadler M, Siddiqui AS, Firestone R, Chandran B. Optimal technology selection and operation of commercial-building microgrids. IEEE Trans Power Syst 2008;23(3):975–82. http://dx.doi.org/10.1109/TPWRS.2008.922654.

[11] Perger T, Auer H. Local energy sharing considering different technologies, individual preferences, and contributions. In: Energy challenges for the next decade, 16th IAEE European conference. International Association for Energy Economics; 2019.

[12] Döci G, Vasileiadou E. Lets do it ourselves individual motivations for investing in renewables at community level. Renew Sust Energy Rev 2015;49:41–50. http://dx.doi.org/10.1016/j.rser.2015.04.051.

[13] Gui EM, MacGill I. Typology of future clean energy communities: An exploratory structure, opportunities, and challenges. Energy Res Soc Sci 2018;35:94–107. http://dx.doi.org/10.1016/j.erss.2017.10.019.

[14] Fina B, Auer H, Friedl W. Profitability of PV sharing in energy communities: Use cases for different settlement patterns. Energy 2019;189:116148. http://dx.doi.org/10.1016/j.energy.2019.116148.

[15] European Commission. Clean energy for all Europeans, Communication from the Commission to the European Parliament, the Council, the European Economic and Social Committee. Committee Region European Investment Bank; 2016.

[16] Inês C, Guilherme PL, Esther M-G, Swantje G, Stephen H, Lars H. Regulatory challenges and opportunities for collective renewable energy prosumers in the EU. Energy Policy 2019;111212. http://dx.doi.org/10.1016/j.enpol.2019.111212.

[17] Heldeweg MA, Saintier S. Renewable energy communities as 'socio-legal institutions': A normative frame for energy decentralization? Renew Sust Energy Rev 2020;119:109518. http://dx.doi.org/10.1016/j.rser.2019.109518.

[18] Brown T, Schlachtberger D, Kies A, Schramm S, Greiner M. Synergies of sector coupling and transmission reinforcement in a cost-optimised, highly renewable European energy system. Energy 2018;160:720–39. http://dx.doi.org/10.1016/j.energy.2018.06.222.

[19] Bloess A, Schill W-P, Zerrahn A. Power-to-heat for renewable energy integration: A review of technologies, modeling approaches, and flexibility potentials. Appl Energy 2018;212:1611–26. http://dx.doi.org/10.1016/j.apenergy.2017.12.073.

[20] Münster M, Morthorst PE, Larsen HV, Bregnbæk L, Werling J, Lindboe HH, et al. The role of district heating in the future Danish energy system. Energy 2012;48(1):47–55. http://dx.doi.org/10.1016/j.energy.2012.06.011.

[21] Good N, Mancarella P. Flexibility in multi-energy communities with electrical and thermal storage: A stochastic, robust approach for multi-service demand response. IEEE Trans Smart Grid 2017;10(1):503–13. http://dx.doi.org/10.1109/TSG.2017.2745559.

[22] Shariatkhah M-H, Haghifam M-R, Chicco G, Parsa-Moghaddam M. Adequacy modeling and evaluation of multi-carrier energy systems to supply energy services from different infrastructures. Energy 2016;109:1095–106. http://dx.doi.org/10.1016/j.energy.2016.04.116.

[23] Skarvelis-Kazakos S, Papadopoulos P, Unda IG, Gorman T, Belaidi A, Zigan S. Multiple energy carrier optimisation with intelligent agents. Appl Energy 2016;167:323–35. http://dx.doi.org/10.1016/j.apenergy.2015.10.130.

[24] Luthander R, Widén J, Nilsson D, Palm J. Photovoltaic self-consumption in buildings: A review. Appl Energy 2015;142:80–94. http://dx.doi.org/10.1016/j.apenergy.2014.12.028.

[25] Gabrielli P, Gazzani M, Martelli E, Mazzotti M. Optimal design of multi-energy systems with seasonal storage. Appl Energy 2018;219:408–24. http://dx.doi.org/10.1016/j.apenergy.2017.07.142.

[26] Alghool DM, Elmekkawy TY, Haouari M, Elomri A. Optimization of design and operation of solar assisted district cooling systems. Energy Convers Manage X 2020;100028. http://dx.doi.org/10.1016/j.ecmx.2019.100028.

[27] Rigo-Mariani R, Wae SOC, Mazzoni S, Romagnoli A. Comparison of optimization frameworks for the design of a multi-energy microgrid. Appl Energy 2020;257:113982. http://dx.doi.org/10.1016/j.apenergy.2019.113982.

[28] Orehounig K, Evins R, Dorer V. Integration of decentralized energy systems in neighbourhoods using the energy hub approach. Appl Energy 2015;154:277–89. http://dx.doi.org/10.1016/j.apenergy.2015.04.114.

[29] Morvaj B, Evins R, Carmeliet J. Optimization framework for distributed energy systems with integrated electrical grid constraints. Appl Energy 2016;171:296–313. http://dx.doi.org/10.1016/j.apenergy.2016.03.090.

[30] McKenna R, Merkel E, Fichtner W. Energy autonomy in residential buildings: A techno-economic model-based analysis of the scale effects. Appl Energy 2017;189:800–15. http://dx.doi.org/10.1016/j.apenergy.2016.03.062.

[31] Prete CL, Hobbs BF. A cooperative game theoretic analysis of incentives for microgrids in regulated electricity markets. Appl Energy 2016;169:524–41. http://dx.doi.org/10.1016/j.apenergy.2016.01.099.

[32] Mengelkamp E, Gärttner J, Rock K, Kessler S, Orsini L, Weinhardt C. Designing microgrid energy markets: A case study: The brooklyn microgrid. Appl Energy 2018;210:870–80. http://dx.doi.org/10.1016/j.apenergy.2017.06.054.

[33] Fichera A, Frasca M, Volpe R. Complex networks for the integration of distributed energy systems in urban areas. Appl Energy 2017;193:336–45. http://dx.doi.org/10.1016/j.apenergy.2017.02.065.

[34] Pinel D. Clustering methods assessment for investment in zero emission neighborhoods' energy system. Int J Electr Power Energy Syst 2020;121:106088. http://dx.doi.org/10.1016/j.ijepes.2020.106088.

[35] Mehleri ED, Sarimveis H, Markatos NC, Papageorgiou LG. A mathematical programming approach for optimal design of distributed energy systems at the neighbourhood level. Energy 2012;44(1):96–104. http://dx.doi.org/10.1016/j.energy.2012.02.009.

[36] Kriechbaum L, Scheiber G, Kienberger T. Grid-based multi-energy systems—modelling, assessment, open source modelling frameworks and challenges. Energy Sust Soc 2018;8(1):35. http://dx.doi.org/10.1186/s13705-018-0176-x.

[37] Groissböck M. Are open source energy system optimization tools mature enough for serious use? Renew Sust Energy Rev 2019;102:234–48. http://dx.doi.org/10.1016/j.rser.2018.11.020.

[38] Ajila SA, Wu D. Empirical study of the effects of open source adoption on software development economics. J Syst Softw 2007;80(9):1517–29. http://dx.doi.org/10.1016/j.jss.2007.01.011.

[39] Bazilian M, Rice A, Rotich J, Howells M, DeCarolis J, Macmillan S, et al. Open source software and crowdsourcing for energy analysis. Energy Policy 2012;49:149–53. http://dx.doi.org/10.1016/j.enpol.2012.06.032.

[40] Dorfner J. Open source modelling and optimisation of energy infrastructure at urban scale [Ph.D. thesis], Technische Universität München; 2016, https://mediatum.ub.tum.de/1285570.

[41] Alhamwi A, Medjroubi W, Vogt T, Agert C. Flexigis: an open source GIS-based platform for the optimisation of flexibility options in urban energy systems. Energy Procedia 2018;152:941–6. http://dx.doi.org/10.1016/j.egypro.2018.09.097.

[42] Wilkinson MD, Dumontier M, Aalbersberg IJ, Appleton G, Axton M, Baak A, et al. The FAIR guiding principles for scientific data management and stewardship. Sci Data 2016;3. http://dx.doi.org/10.1038/sdata.2016.18.

[43] Barnes N. Publish your computer code: it is good enough. Nature 2010;467(7317). 753–753.

[44] Barba LA. The hard road to reproducibility. Science 2016;354(6308). http://dx.doi.org/10.1126/science.354.6308.142, 142-142.

[45] Wilson G, Bryan J, Cranston K, Kitzes J, Nederbragt L, Teal TK. Good enough practices in scientific computing. PLoS Comput Biol 2017;13(6). http://dx.doi.org/10.1371/journal.pcbi.1005510.

[46] OpenStreetMap contributors. Map section of vienna, Austria. OpenDatabase license ODbL. 2020, http://creativecommons.org/licenses/by-sa/2.0/.

[47] Stadt Wien - Straßenverwaltung und Straßenbau (MA 28). Digitaler Zentraler Leitungskataster (ZLK). 2020.

[48] EEG-EC. Energy community technology database. Internal database at energy economics group (EEG) at Vienna university of technology. 2020.

[49] Ahlgren E, Simbolotti G, Tosato G. District heating. Energy Technol Sys Anal Program Technol Brief E 2013;16.

[50] WU (Wirtschaftsuniversität). Umwelterklärung 2019. 2019, https://www.wu.ac.at/fileadmin/wu/h/structure/servicecenters/procurement/Umwelt/Umwelterklaerung19_web_final.pdf.

[51] Vogl F. Alternative Wege in der Energieversorgung von Standorten. BauConsult Energy GmbH; 2019, https://nachhaltigwirtschaften.at/resources/sdz_pdf/events/20190131-tws-sdz/03_Vogl_KWK_Viertel_Zwei.pdf?m=1549984836&.

[52] Schieferdecker B, Funfgeld C, Meier H, Adam T. Repräsentative VDEW-Lastprofile. 1999, VDEW-Materialien M-28/99, Frankfurt.

[53] BGW. Praxisinformation P 2007/13 gastransport/betriebswirtschaft: Abwicklung von standardlastprofilen. 2007.

[54] MINES ParisTech/Transvalor. Irradiation values from helioclim-3 and meteorological data (MERRA-2 and GFS): generated using copernicus atmosphere monitoring service information 2016. 2018.

[55] ZAMG. Meteorologische messdaten der ZAMG. 2012–2018. 2018, https://creativecommons.org/licenses/by/3.0/at/deed.de.

[56] Lindberg KB, Doorman G, Fischer D, Korpås M, Ånestad A, Sartori I. Methodology for optimal energy system design of zero energy buildings using mixed-integer linear programming. Energy Build 2016;127:194–205. http://dx.doi.org/10.1016/j.enbuild.2016.05.039.

[57] E-Control. Suppliers and prices. 2018, https://www.e-control.at/en/preise-vergleichen-lieferanten-auswahlen.

[58] Rademakers K, Smith M, Yearwood J, Saheb Y, Moerenhout J, Pollier K, et al. Study on energy prices, costs and subsidies and their impact on industry and households. 2018, http://dx.doi.org/10.2833/825966.